

26th Seismic Research Review - Trends in Nuclear Explosion Monitoring

USING GROUND TRUTH EVENTS FOR TRAVEL TIME CALIBRATION AND STUDYING SEISMIC ENERGY GENERATION AND PARTITIONING INTO VARIOUS REGIONAL PHASES

Yefim Gitterman¹, Vladimir Pinsky¹, Kyriakos Solomi², Rami Hofstetter¹, Cemil Gurbuz³, and Mehmet Ergin⁴

Geophysical Institute of Israel¹, Geological Survey Department of Cyprus², Bogazici University³, Kandilli Observatory and Earthquake Research Institute⁴, and TUBITAK Marmara Research Center⁵

Sponsored by Defense Threat Reduction Agency and Air Force Research Laboratory

Contract No. DTRA01-01-C-0119¹ and FI962 -03-C-0124²

ABSTRACT

On-land seismic calibration explosions were recently conducted in Cyprus complementary to a previous calibration series at Rotem quarry, Israel. The experiment's goal was to improve our models for calculating travel times of seismic waves to local and regional seismic stations, and to contribute to the study of explosion source phenomenology in specific geological settings. A preliminary shot of 300 kg and the subsequent main calibration shot of 2,000 kg were conducted in the same deep (~200 m) borehole full of water located in the diabase massif in the Macheras Forest. Both explosions were accompanied by a series of water fountains and gas emissions in the air of more than 100 m in height for 10-30 seconds. The explosions produced much higher frequency seismic energy than the Dead Sea and Rotem calibration shots, which resulted in rapid signal attenuation with distance. Strong seismic signals with prominent P first arrivals dominant over weak S waves were observed at the close broadband (BB) station CSS (~20Hz at distance ~10 km). Peak frequencies and spectral shape were nearly identical for both calibration shots, only amplitudes increased for the larger shot (4-5 times). The relatively low seismic strength and the invariance of spectral content with charge size were due to the placement in a deep borehole in diabase filled with water. High-frequency P-signals can be still found after narrow-band filtration at some remote (up to 300 km) portable stations deployed by TUBITAK and KOERI in Turkey. The explosions, the first conducted for calibration of Cypriot stations, contributed to the improvement of the crustal velocity model in the Eastern Mediterranean and the characterization of seismic signal attributes of this unique source for nuclear monitoring identification.

Spectral ratios of Pg and Lg waveforms were used to investigate source-scaling relations for different pairs of explosions in Cyprus and Israel (Rotem quarry), and to estimate the source corner-frequency dependence on yield. We complemented the ground truth (GT) database by new GT0-GT5 events which occurred before and during the project, and also by GT10 cluster events, and verified newly computed source-specific station corrections (SSSCs) using this additional data. The database was enriched by GT5 events from east Turkey, Lebanon, southern and eastern Iran and Israel. New event clusters, from aftershocks of the Bingol, Turkey (M=6.4, May 1, 2003), and Dead Sea (ML=5.2; February 11, 2004) earthquakes, were collected and characterized.

The series of aftershocks from the Dead Sea earthquake were relocated using the AUTOLOC non-linear algorithm, and used for validation of the local travel time model obtained from calibration explosions in the Dead Sea in 1999 and for establishing empirical travel time corrections (ETTCs) for the Israel Seismic Network and the International Monitoring System (IMS) array AS049 on Mt. Meron. A subset of 10 aftershocks together with a number of regional earthquakes, recorded by the array, was used for tuning the newly designed ROBTEAM algorithm. The algorithm showed considerably better performance than conventional beamforming.

We computed 3D CUB1.0 model-based SSSCs for the IMS stations EIL, MRNI, KEG and BRAR and compared these SSSCs with ETTC from the relocation experiment and raw waveform pickings for different seismic phases. For a subset of the source-station travel time corrections the model based SSSCs were in good agreement with ETTCs, however large discrepancies were also observed. We then digitized the regionalization map of Sweeney and Walter (1998) and utilized the new Global Moho model of Barazangi and Sandvol (2001) to construct a modified model MCUB1. The new model shows less discrepancy between the ETTCs and SSSCs and was used as a starting point in a trial and error process for construction of the best-fit GCUB1 model. This model has been validated by travel time computations from the two large GT5 Izmit (August 17, 1999) and Bingol earthquakes in Turkey.

26th Seismic Research Review - Trends in Nuclear Explosion Monitoring

OBJECTIVE

The main objectives of the projects are: 1) determination and verification of empirical source scaling relationships, estimation of seismic efficiency and comparison of different calibration explosions; 2) quantifying the coupling and specific seismic source features, including energy generation analysis and energy partitioning into various regional phases; 3) collection of regional Ground Truth data GT0-GT5; 4) improvement and automation of event monitoring by development and application of advanced methods; 5) calibration of seismic travel times at local and regional distances in the Middle East and East Mediterranean region.

RESEARCH ACCOMPLISHED

Cyprus calibration experiment

GSD and GII conducted two experimental explosions in a deep borehole in the nature reserve of Macheras Forest, Cyprus (Figure 1). The borehole was placed in a diabase hard rock massif and filled with water, providing good stemming, and favorable factors for good coupling and a strong seismic signal. Ground Truth parameters and charge design of the explosions are presented in Table 1 and Figure 2.

First, we conducted a test explosion of 300 kg of dynamite. During this test we checked all logistics, timing, and explosive downloading operations. We measured ground vibrations at close distances and estimated that the ground vibration level during the main calibration explosion would be safe for nearby churches and monasteries (see Figure 1).

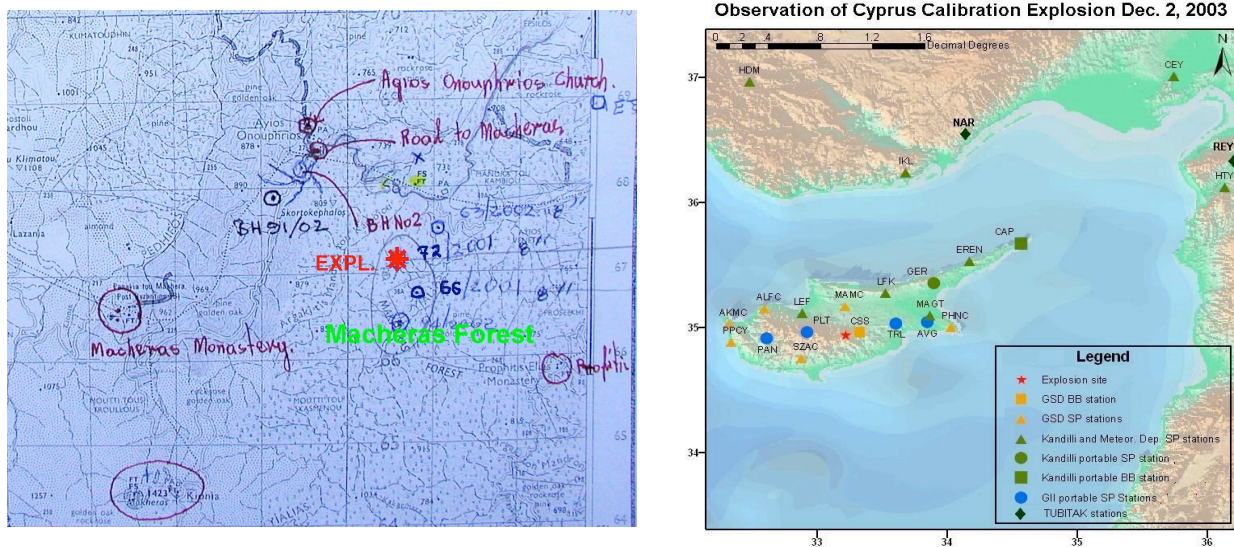


Figure 1. Location of Cyprus experimental explosions (left) and recording stations (right).

Table 1. Ground truth parameters of Cyprus explosions

Date	Borehole #	Coordinates Latit. Long.	Origin Time, GMT	Charg e, kg	Hole depth, m	Water level, m	Charge length, m
17.11.03	BH72/01	34.94604°N	13:17:23.17	300	213	9.5	8
2.12.03	203 mm	33.22509°E	13:00:00.92	2000	208		26

The test shot did not damage the borehole, so the main calibration explosion of 2000 kg of dynamite was detonated in the same borehole refilled with ground water. The charge length (26 m) was less than expected (53 m), possibly due to a cavity created during the test shot (see Figure 2).

Video-record analysis showed that the explosion was followed by three water fountains separated by 7-8 sec, and gas emission into the air (total duration ~2 min) to a height of more than 100 m (Figure 3).

26th Seismic Research Review - Trends in Nuclear Explosion Monitoring

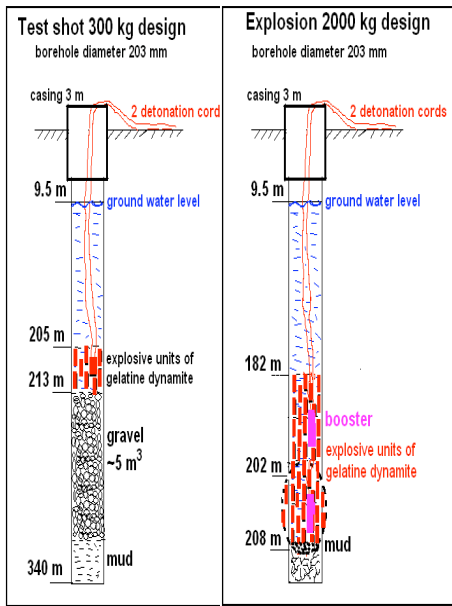


Figure 2. Charge design for the explosions (in the same borehole). For the 2-ton explosion the charge length (26 m) was less than expected (53 m), due to a cavity created during the test shot.



Figure 3. Water fountains during the test shot (left) and the 2-ton explosion (right), snapshots from a remote video-camera placed at the top of a nearby hill in Macheras forest.

For the explosions GSD and GII deployed a number of strong motion instruments at close range: 3 vibration sensors (at the same sites for both shots) and 3 accelerometers, to provide high-quality records of seismic radiation (Figure 4) for characterization of the specific source phenomenology.

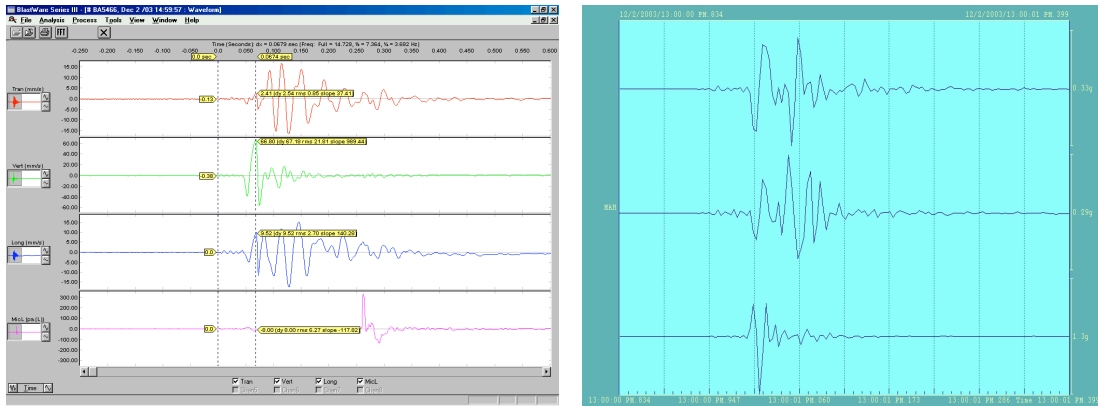


Figure 4. Records of radiated signals from the 2-ton shot at the closest epicentral distances: BlastMate III velocity sensors at ~100 m (left); and accelerometer at ~90 m, maximal vertical acceleration 1.3g (right).

Ground vibration records at close distances revealed large peak particle velocities, 2-3 times more than the values measured for calibration explosions at Rotem quarry, Israel (Gitterman et al, 2002), but at much higher frequencies (40-60 Hz). A maximal vertical peak velocity of 67 mm/sec was observed from the 2-ton explosion, ~1.7 times larger than for the test shot. Three accelerometers with GPS timing located at epicentral distances of 90-1900 m supplied good signals in the range 0.006-1.3g (Figure 4). These close-in records and impressive video observations suggest that the explosives detonated completely, resulting in increased amplitudes.

Strong high-frequency (~20 Hz) seismic signals, observed at the close BB station CSS, with prominent first P-arrivals, dominant over weak S waves, are similar for both explosions (see Figure 5). For the almost 8-times larger 2

26th Seismic Research Review - Trends in Nuclear Explosion Monitoring

ton charge the dominant frequency f_0 should decrease at least a factor of 2 times according to theoretical considerations: $f_0 \sim k/W^{1/3}$. Surprisingly, waveform, spectral shape and peak frequencies did not change for the larger shot as estimated; only amplitudes were increased (~5 times) as expected.

We hypothesize that the system “dynamite charge in deep borehole filled water + strong hard rock diabase massif” behaved like a resonator tuned to a specific high frequency, independent of power of excitation.

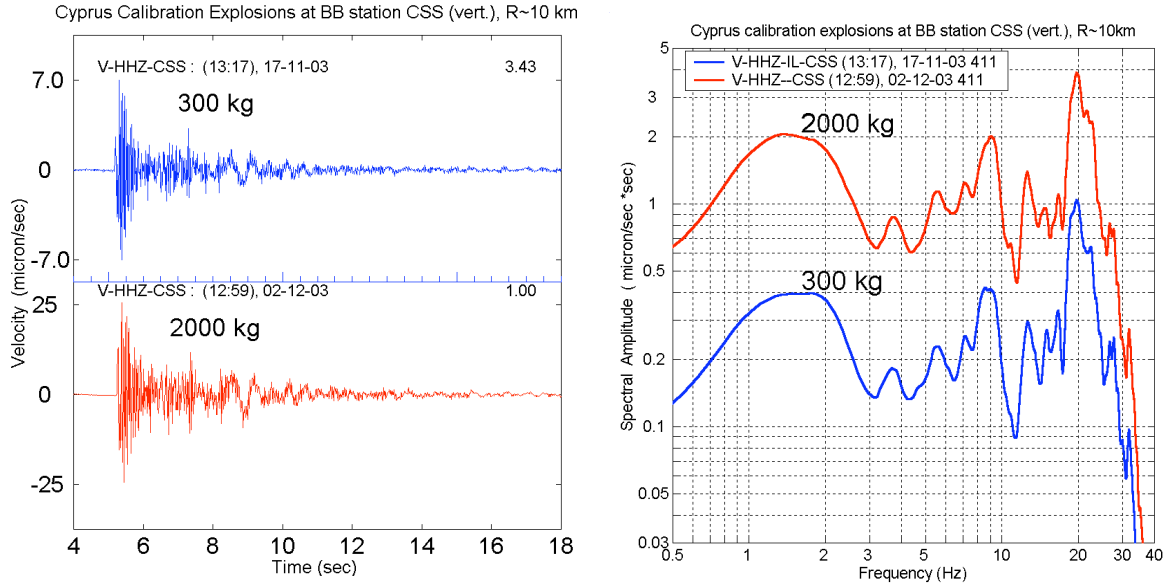


Figure 5. Comparison of waveforms and spectra of the whole signal (~ 10 sec) for the test and calibration explosions at CSS station.

GII, Kandilli Observatory and TUBITAK installed a number of portable short-period stations in Cyprus and Southern Turkey (see map in Figure 1). The large explosion was recorded by most of the Cyprus Seismic Network stations and several portable instruments, including a few stations in Turkey. At many stations the signal-to-noise ratio is low and signal can be found only after narrow band-pass filtration. The local magnitude of the explosion was estimated as $M_L \leq 2$, lower than predicted ($M_L \sim 2.3-2.5$) from the high-coupling factors (fully-contained, explosives in water, hard rocks). However, it is known that deeper burial of a charge can result in decreasing seismic strength (e.g. Leith and Kluchko, 1998). The rapid attenuation of seismic energy with distance can be related to the unexpected very high-frequencies of the radiated signal, much higher than for the Dead Sea and Rotem calibration shots (Gitterman et al. 2002).

Construction of 1D velocity model for Cyprus.

The first Pg and Pn arrivals from the 2-ton explosion to the stations deployed in Cyprus and Turkey have been used to upgrade the existing velocity model by the modified Marquardt-Levenberg optimization procedure. An initial residual RMS=0.9 s for the routine GSD velocity model was reduced to RMS=0.48 as a result of the procedure. The station distribution, P travel time curves before and after the data fitting, and the initial and final P waves velocity models are shown in Figure 6. The new model differs from the previous one by essentially higher velocities in the upper crust, which changed from 4.3 to 5 km/s at $H < 3$ km range and from 5.5 to 6.3 km/s in the depth range 4–10 km. The early P arrivals to the stations AVG and ALFC on opposite sides of Cyprus and the higher velocity model agree with the overthrust ophiolite structure of Cyprus, with its gravity anomaly (Makris & Wang, 1994).

26th Seismic Research Review - Trends in Nuclear Explosion Monitoring

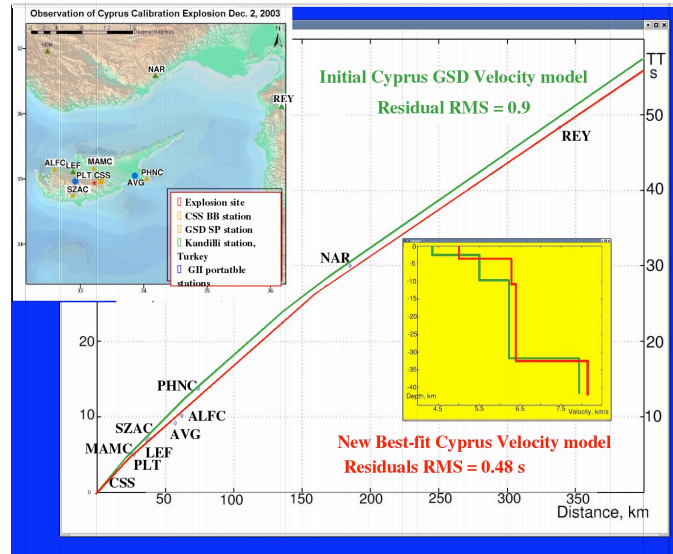


Figure 6. Velocity model construction for Cyprus.

Source Scaling

Amplitude spectra of P and S waveforms were used to investigate source scaling relations for the pair of Cyprus explosions, ideally placed at the same point, recorded at BB station CSS (Figure 7). We used the procedure based on spectral ratios of a pair of explosions of different yield to estimate source corner frequencies (Stump et al., 2003); we extracted also corner frequency estimates from the results presented in this paper for nearly contained blasts in a mine in Wyoming, recorded at the Pinedale array.

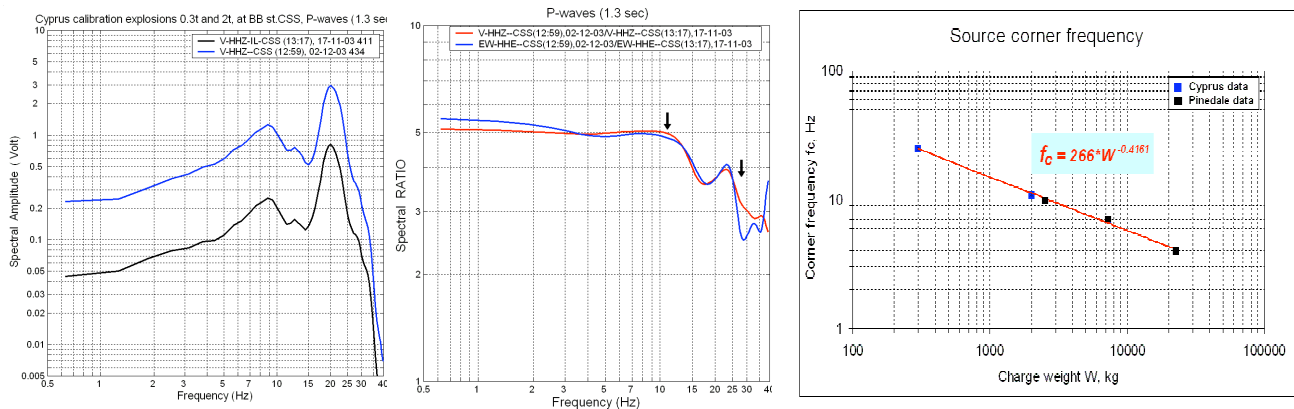


Figure 7. Smoothed amplitude spectra of P-wave portion for the pair of Cyprus explosions (left) were used to calculate spectral ratios for vertical and radial components and estimate corner frequencies from the ratios (middle); these estimates together with values from Stump et al. (2003) were used to compute a regression curve (right).

The Cyprus explosions can be undoubtedly considered fully contained despite impressive external effects. Both datasets showed consistency in spite of the different conditions: charge design, scaled depth, geological settings, distances. This leads to a good fit for the empirical corner frequency-yield relation:

$$f_c = 266 * W^{-0.4161}$$

Sayarim experiment

Experimental explosions of 0.3, 2 and 32.5 ton of ANFO were conducted recently in Sayarim Valley near Eilat, Israel, providing a series for yield-dependent analysis of regional waveforms (Figures 8, 9). The large shot,

26th Seismic Research Review - Trends in Nuclear Explosion Monitoring

considered as a calibration explosion, was mostly supported by the MERC program of the U.S. AID. Explosives were placed in boreholes of large diameter (0.6-0.8 m) with depth of 17-21 m, drilled in dry Quaternary alluvial conglomerates. A seismic refraction survey was conducted before the experiment on the site; P-velocity ~1670 m/sec was found for the layer that accommodated the charges.

Good waveform records were obtained for the explosion series in the near-source region by accelerometers at distances 100-500 m, and numerous portable and network seismic SP and BB stations, up to ~400 km. Significant seismic excitation was achieved ($M_L \sim 2$ for 2 ton and $M_L \sim 3$ for 32.5 ton) in spite of the non-consolidated sediment shot medium - dry alluvium, commonly considered a low-coupling material (e.g., US Congress, 1988). Comparison with the Rotem experiment results (Gitterman, 2002) does not show any significant magnitude drop (Figure 10). All available regional data (Jordan, Saudi Arabia) will be collected and analyzed jointly with the close-in records.



Figure 8. Ground uplift for the 2-ton explosion (video snapshot ~1 sec after detonation).



Figure 9. View of the largest explosion.

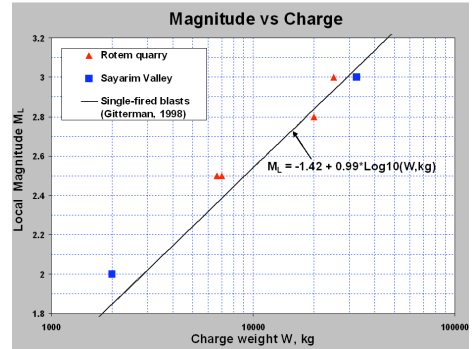


Figure 10. Local magnitude vs charge weight dependence for simultaneous explosions.

5. GT5–Ground Truth Database.

This database was enriched by one candidate GT5 event from East Turkey, and three from Israel. The GT data for these four events is presented in Table 2. The main shock and aftershocks around Bingol, Turkey ($M=6.4$, May 1, 2003) (see Figure 11, Table 2, event 2), were collected and characterized, using data from the Kandilli observatory network and two portable networks deployed promptly after the large event: 10 stations of the joint deployment of GFZ (Potsdam) and ERD (Ankara) and 6 temporary stations of the TUBITAK deployment (see Figure 12). The event has a good coverage by the Kandilli network, which together with the temporary deployments delivers 90% GT5 criterion certification to the event. Unfortunately both portable deployments do not close an azimuthal gap to the North of the event.

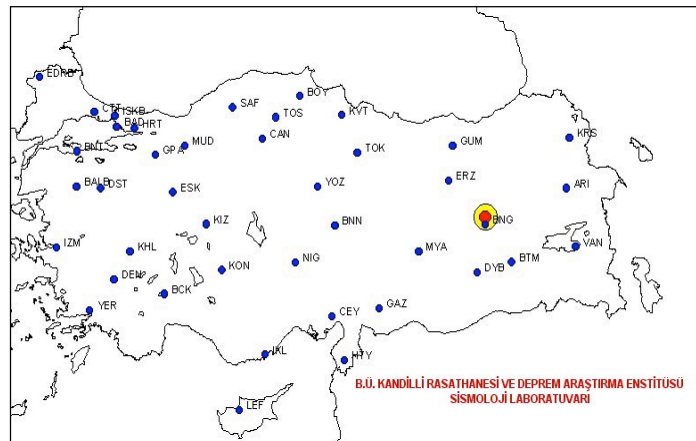


Figure 11. Distribution of Kandilli observatory stations, reporting Bingol main shock.

26th Seismic Research Review - Trends in Nuclear Explosion Monitoring

Table 2. New candidate GT5 event collection.

Event number	yy mm dd	hh:mn:sd	M	Lat	Lon	dx	dy	H km	Min R, km	Gap1	Gap2
1	94 08 16	03:18:57.2	4.0	32.046	35.500	3.3	2.1	18.0±8.1	19	79°	88°
2	03 05 01	00:27:04.5	6.4	39.004	40.435	2.6	2.2	6.0	10	100°	170°
3	04 02 11	08:15:03.2	5.2	31.706	35.550	2.0	0.9	16.0±1.6	14	68°	98°
4	04 07 07	14:35:08.7	4.7	31.979	35.546	4.0	0.3	14.0±2.9	30	72°	94°

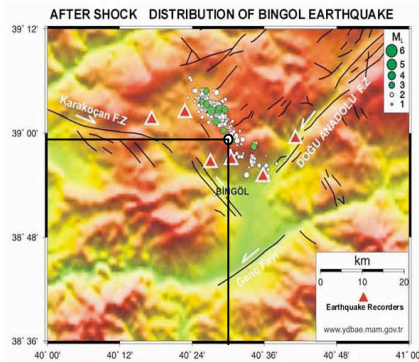


Table 3. Aftershocks list M > 4.

Event number	M	D	H	M	Sc	Lat	Lon	Dep	M _L
1	05/10	23	41	40.6		39.065	40.469	4.8	4.0
2	05/08	01	44	19.2		39.095	40.437	5.4	4.6
3	05/10	15	44	49.4		39.079	40.442	3.8	4.4
4	05/05	06	05	27.5		38.987	40.505	6.9	4.3
5	05/12	04	10	08.9		39.022	40.497	5.3	4.0
6	05/04	02	09	56.4		39.043	40.453	5.5	4.0

Figure 12. Aftershocks of the Bingol earthquake M=6.4, recorded by the TUBITAK portable network

A set of the relatively strong aftershocks has been recorded in the close vicinity of the temporary network stations. For example, event 3 (Table 3) was recorded by station SUD with $T_s-T_p=0.6$ sec, giving distance to the hypocenter within 5 km (see Pinsky et al., 2003a). The event was also registered by the TUBITAK portable network, by the Kandilli network, reported to the EMSC and also by the IDC. TUBITAK reports about six events $M>4$ in the area (see Figure 12 and Table 3), particularly, event 4 occurred very close to stations B06 and B03 of the TUBITAK portable network. The Bingol cluster candidate GT5 events may be very useful for site specific station calibration.

Two recent significant earthquakes within the Israel and Jordan seismic networks were collected: the $M_L=5.2$ Dead Sea earthquake (Figure 13, Table 2, event 3) and the $M_L=4.7$ Jordan Valley earthquake (Table 2, event 4). Both of them satisfy the GT5 candidate event selection criteria at the 95% confidence level.



Figure 13. The Dead Sea, Israel ($M_L=5.2$, December 11, 2004) earthquake, located at the 95% level of the GT5 selection criteria (left) was detected at large distance, providing useful calibration information to a number of IMS stations (right, from the IDC Website). The Dead Sea earthquake (★) was followed by a swarm of aftershocks (●), shifted slightly to the north-west (left). The green star (★) indicates location of the earthquake, using the AUTOLOC procedure.

26th Seismic Research Review - Trends in Nuclear Explosion Monitoring

The earthquake location has been tested using the relocation approach (Pinsky et al, 2003a) and P and S arrival times to the ISN, JSN and IMS stations within 2500 km (including the new AS049 array and the ASF station). The P and S travel times have been calculated according to the ISAPEI91 model and compared to the measured times for computation of Empirical Travel Time Corrections (ETTCs). Theoretical reciprocal SSSCs according to the CUB1 and CUB2 models (Barmin et al, 2001) and the newly designed NCUB1 and MCUB1 (Pinsky et al, 2003a) have been calculated for SSSC and ETTC comparison. For the earthquake calibration information, contact vlad@mni.gov.energy.il.

The Shomron Region (Israel) earthquake, $M_L=4.1$, 1994/09/16 03:18:57 was located during the Joint Seismic Observation Period Experiment (JSOP-1) carried out during September-November, 1994 by several Eastern Mediterranean networks. The minimum distance of 19 km, primary gap $\text{Gap1}=79^\circ$ and secondary gap $\text{Gap2}=88^\circ$ attribute this event to the 95% GT5 class.

IMS station KEG calibration due to the GT5 events.

We analyzed the GT5 reference event list (McLaughlin, 2003) for calibration of KEG. The P arrivals were picked at GII using the BB KEG seismograms. From the initial list of 55 events, only 18 have been chosen (Pinsky et al, 2003a), because of poor SNR or large time misfit. The data consists of the two main clusters and two separate events (see Figure 14).

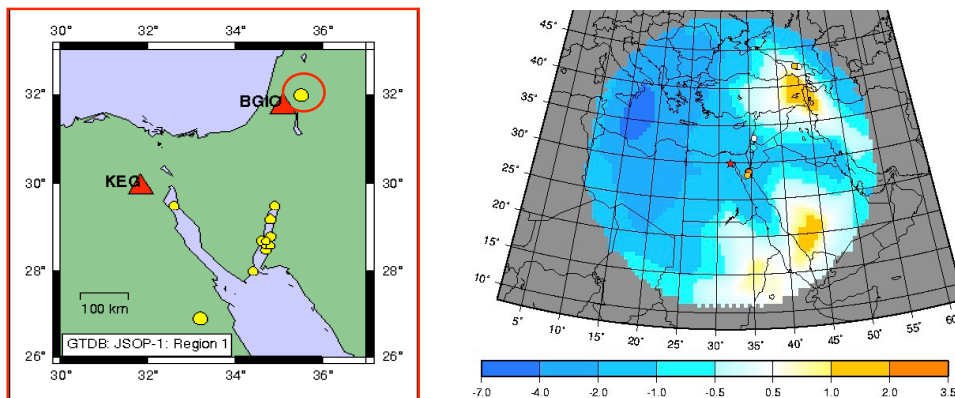


Figure 14. KEG calibration reference events from the JSOP-1 experiment (left) and CUB1.0 model SSSCs (contours) compared to empirical TT corrections (points), obtained from the set of GT5 events (right).

One cluster around $\text{Lat}=42.4$, $\text{Lon}=43.7$ comprises Caucasus events, the second ($\text{Lat}=28.5$, $\text{Lon}=34.6$) is the Gulf of Aqaba set. Two separate earthquakes: north of the Dead Sea, and Golan Heights, show satisfactory fit between ETTCs and the SSSCs of CUB1.0. The Caucasus events are in average in satisfactory agreement with the model. But the Gulf of Aqaba clusters deviate far from the model and even from each other.

CUB1.0 upgrading within the Middle East, Eastern Mediterranean Region.

The map of Sweeney and Walter, (1998, Figure 15) was taken for construction of a digitized $1^\circ \times 1^\circ$ grid 1D crust model within the given boundaries. A new global model NCUB1 (Pinsky et al, 2003a) was determined by substitution of this new digital crust for the CUB1.0 crust. SSSCs for the given regional IMS stations EIL, MRNI, BRAR, KEG, KVAR, MLR have been calculated using the Barmin 2D raytracer utility and compared to the empirical ETTCs, obtained via thorough seismogram analysis, re-picking and relocation of the collected regional GT events (Pinsky et al, 2003a). An additional modified model MCUB1 was constructed by introduction of Global Moho depth information (Barazangi and Sandvol, 2001). Empirical travel times are assumed fitting a model, if $|\text{ETTC-SSSC}| < 1$ sec. The number of fitted ETTCs versus the total number of existing GT5 events for the IMS stations is presented in Table 4.

26th Seismic Research Review - Trends in Nuclear Explosion Monitoring

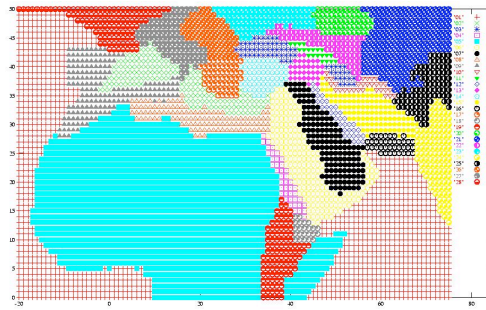


Figure 15. Digital regionalization map, computed according Sweeney and Walter, 1998

Table 4. Pn Model Travel Time Corrections versus Empirical Travel Time Corrections.

STATION NAME /MODEL	EIL	MRNI	BRAR	MLR	KVAR	DAVOS	GERESS	OBN	Σ
CUB1	4/8	3/5	2/4	3/5	3/5	0/2	1/4	3/3	18/35
NCUB1	6/8	5/5	4/4	5/5	4/5	1/2	4/4	3/3	32/35
MCUB1	5/8	4/5	4/4	3/5	4/5	1/2	4/4	3/3	28/35

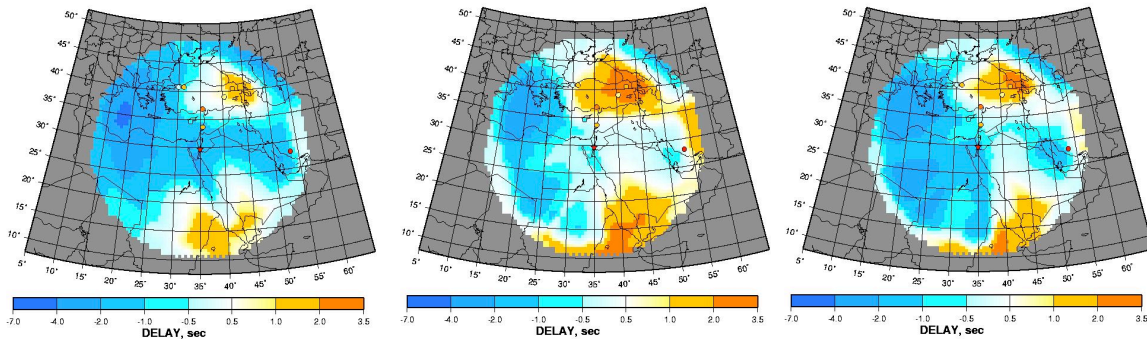


Figure 16. Pn SSSCs and ETTCs for depth H=10 km for station EIL using the CUB1.0 model (left), NCUB1 (centre) and MCUB1 (right).

Figure 16 demonstrates the computation results for station EIL. Map color indicates $(T_{\text{model}} - T_{\text{iaspei91}})$ residuals, circles show the GT5 event locations and their color corresponds to the ETTCs. Table 4 and Figure 16 show that by application of NCUB1 and MCUB1 we generally improve the fit between the model SSSCs and ETTCs. For example, the EIL observations of Duzce, Izmit, S. Iran and Lebanon events better fit NCUB1 and MCUB1 than CUB1.0. The fitting is significantly improved for the stations BRAR and MLR (see Pinsky et al, 2003a) for all available observations. However, several cases of discrepancy between SSSCs and ETTCs are still present.

Travel time improvements by NCUB1 are demonstrated in Figure 17, where $(T_{\text{obs}} - T_{\text{calc}})$ histograms for the IMS stations are shown for the GT5 Izmit earthquake of August 17, 1999, M=7.1. Due to the station configuration and location results the earthquake is a candidate GT5 event at 95% confidence level. The NCUB1 model removes the bias of 0.91 sec provided by the CUB1.0 model with almost the same standard deviation.

26th Seismic Research Review - Trends in Nuclear Explosion Monitoring

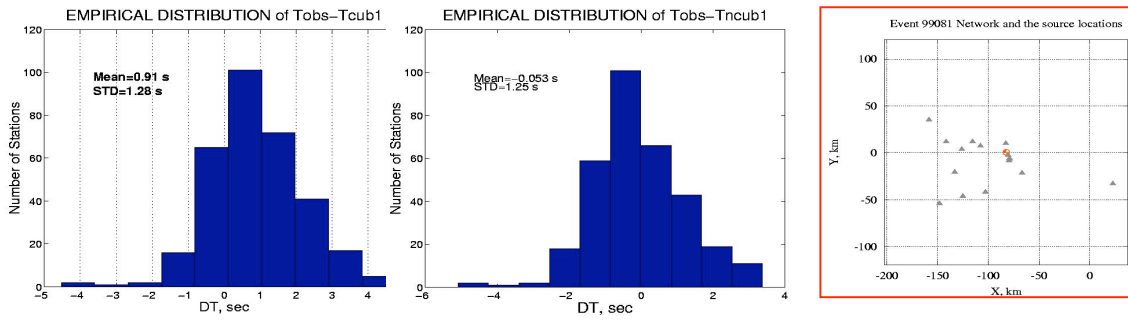


Figure 17. Empirical distributions of Tobs-Tcalc (P first arrival) for the Izmit earthquake, calculated for all relevant regional stations using CUB1.0 (left) and NCUB1 (center) models. Local Network configuration (right) provides 95% confidence level (GT5) for the event.

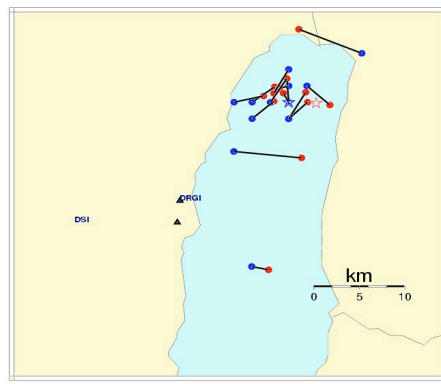


Figure 18. Aftershock location by the AUTOLOC (●) and analyst solutions (●).

Dead Sea Earthquake Series Advanced Location Study.

The February 11, 2004 earthquake of $M_L=5.2$ was followed by a series of aftershocks with magnitudes $M_L=2$ and less. The earthquake swarm was utilized for testing and calibration of advanced location procedures AUTOLOC and RBEAM (Pinsky et al, 2003b), being developed at GII. AUTOLOC (Pinsky, 2000) is a sophisticated procedure, based on automatic P and S phase picking and robust non-linear grid-search location. The algorithm provides automatic weighting of the pick data: enhancing good fit data and eliminating outliers for location. Persistently deviating first arrivals are accumulated for following station corrections. Figure 18 shows that 10 of 12 earthquakes have been located automatically by the AUTOLOC procedure within 3 km of the GII analyst solutions. For two events the error is somewhat greater, due to poor network configuration and low SNR at first arrivals for these events.

Waveforms of the earthquake series were also used for source location by the new 16 element seismic array on Mt. Meron and its calibration. The new robust beamforming algorithm RBEAM (Pinsky et al, 2003b) was tested using this data, showing advantages over the conventional beamforming and F-K analysis (see Figure 19 and Table 5).

Table 5. Comparison between RBEAM and Beam Azimuth estimations for 6 aftershocks.

Event N	1		2		3		4		5		6		Standard deviation
	Az	Err											
Beam	161°	12.7°	185°	11.4°	189°	15.2°	171°	-3.4°	168°	-6.6°	163°	-11.5°	10.8°
Rbeam	172°	-1.7°	174.5°	-0.1°	171°	-3.8°	174°	-0.4°	176°	2.4°	175°	0.5°	1.98°
“True Az”	173.7°		174.6°		174.8°		174.4°		174.6°		174.5°		

26th Seismic Research Review - Trends in Nuclear Explosion Monitoring

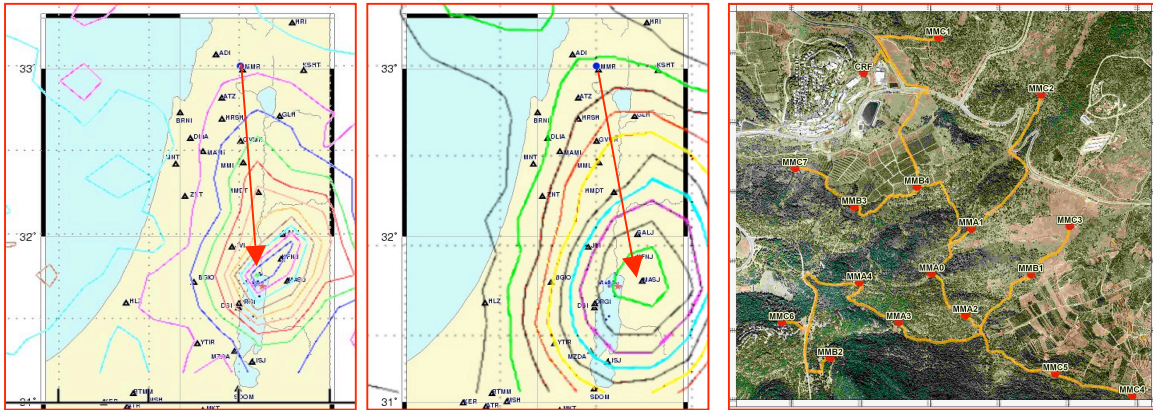


Figure 19. Wavenumber K_x , K_y domain solution, using RBEAM (left) and conventional beamforming (central) for the Dead Sea main shock recorded by AS049 array (right).

CONCLUSIONS AND RECOMMENDATIONS

GII jointly with GSD successfully conducted an on-land seismic calibration explosion series in Cyprus. The unique source parameters (two shots of different charge in the same deep borehole filled with water in a diabase massif) supplied valuable close-in and regional observations. The data were used for a source scaling study, including estimations of corner frequency by the spectral ratio procedure and determination of a simple empirical corner frequency-charge relationship. To check the potential of this analysis for yield estimation it is necessary to accumulate appropriate data from other experimental series of contained explosions. The calibration explosion helped to obtain an improved velocity model for the Cyprus area.

GII conducted a yield-dependent series in Sayarim Valley, Israel, to study energy generation from regional phases. Significant seismic excitation was achieved in spite of non-consolidated sediment media - dry alluvium, commonly considered a low-coupling material, and the shallow burial, far from fully-contained, conditions. All available regional data (Jordan, Saudi Arabia) will be collected and analyzed jointly with close-in accelerometer records.

We have supplemented the reference events data base by a number of GT5 candidates from new sites, evaluated ETTCs for the regional IMS stations and compared them to SSSCs from the CUB1.0 and two new models NCUB1 and MCUB1, demonstrating higher regional accuracy. The new models will be further developed and validated using reliable GT data including recent reference events within the Israel and Jordan Networks.

The new robust beamforming technique RBEAM showed significant advantages over conventional beamforming, using aftershock data from the large event in the Dead Sea in February, 2004. Further investigation is necessary for calibration of the new IMS array AS049, using the RBEAM technique, including a large statistical experiment to estimate the effectiveness of the new approach in various conditions.

The Dead Sea swarm was advantageous for an AUTOLOC procedure test. The algorithm is a non-linear grid-search location routine providing separation of well fitting data and outliers carrying information useful for station calibration.

REFERENCES

- Barazangi M. & Sandvol E. (2001), Calibration of the Selected IMS stations in the Middle East to Improve Seismic Event Location, (contract 00/20/5019 CTBTO/IDC Calibration Programme – Phase 1).
- Barmin, M.P., M.H. Ritzwoller, and A.L. Levshin (2001), A fast and reliable method for surface wave tomography, *Pure Appl. Geophys.*, 158(8), 1351 - 1375.

26th Seismic Research Review - Trends in Nuclear Explosion Monitoring

- Gitterman, Y. (1998), Magnitude-yield correlation and amplitude attenuation of chemical explosions in the Middle East, Proceedings of the 20th Annual Seismic Research Symposium on Monitoring a Comprehensive Nuclear Test Ban Treaty, Santa Fe, Sept.21-23, 1998, 302-311.
- Gitterman, Y., V. Pinsky, A. Shapira, M. Ergin, D. Kalafat, G. Gurbuz, K. Solomi (2002), Improvement in detection, location and identification of small events through joint data analysis by seismic stations in the Middle East/Eastern Mediterranean region, Proceedings of the 24th Seismic Research Review, Ponte Vedra Beach, Sept. 17-19, 2002.
- Leith, W. and L. Kluchko (1998), Seismic Experiments, Nuclear Dismantlement Go Hand in Hand in Kazakhstan, *Eos Trans. Am. Geophys. Union*, 79, 437, 433-444.
- Makris J. and J. Wang (1994), Bougier gravity anomalies of the Eastern Mediterranean Sea. In Geological Structure of the Eastern Mediterranean, Historical Productions-Hall Ltd 1994.
- McLaughlin (Editor) (2003), Source Specific Station Corrections (SSSCs) for Monitoring Seismic Stations in North Africa, Middle East and Western Asia, Group 2. Final Report - Contract DTRA01-00C-0013.
- Pinsky V., Y. Gitterman, V. Goldshmidt, A. Shapira (2003a), Collection of regional calibration data within the area around the Israel Seismic Network. CTBTO Calibration Program - Phase 1, Final Report- Contract 00/20/5024.
- Pinsky V., Y. Gitterman, A. Shapira, M. Ergin, C. Gurbuz. (2003b), Improvements in Monitoring of Small Regional Events Based on Ground Truth Data in Turkey and Israel. Proceedings of the 25th Seismic Research Review, Tucson, Arizona, September 23-25, 2003.
- Pinsky, V. (2000), Prototype autonomous earthquake locator for regional networks, *Geophysical Research Letters*, Vol. 27, No. 21, 3549-3552.
- Stump, B., D.C. Pearson and V. Hsu (2003), Source scaling of contained chemical explosions as constrained by regional seismograms, *BSSA*, 93, 1212-1225.
- Sweeney J.J, W.R. Walter (1998), Preliminary Definition of Geophysical Regions for the Middle East and North Africa. LLNL report. UCRL-ID-132899.
- U.S. Congress (1988), Office of Technology Assessment, Seismic Verification of Nuclear Testing Treaties, OTA-ISC-361 (Washington, DC: U.S. Government Printing Office, Chapter 6, May 1988).